Journal of Electrocardiology 90 (2025) 153933

Contents lists available at ScienceDirect

Journal of Electrocardiology

journal homepage: www.jecgonline.com

F-wave sway in paroxysmal and chronic atrial fibrillation

Agnese Sbrollini [a], Massimo W. Rivolta [b], Peter Van Dam [c], Elisabetta Viani [d], Micaela Morettini [a], Roberto Sassi [b], Laura Burattini [a,*], Emanuela T. Locati [d,e]

[a] Department of Information Engineering, Università Politecnica delle Marche, Ancona, Italy
[b] Dipartimento di Informatica, Università degli Studi di Milano, Milan, Italy
[c] Center for Digital Medicine and Robotics, Jagiellonian University Medical College, Krakow, Poland
[d] Studio Cardiologico Locati, Milan, Italy
[e] Department of Arrhythmology and Electrophysiology, IRCCS Policlinico San Donato, San Donato Milanese, Milan, Italy

ARTICLE INFO

Keywords:
Vectorcardiography
Atrial fibrillation
Fibrillatory waves
Atrial depolarization

ABSTRACT

Vectorcardiography (VCG) can evaluate the vector loops of electrocardiographic waves, being a time-spatial representation of the heart vector into the three orthonormal leads. During atrial fibrillation (AF), F waves reflect the disorganized depolarization of the atria, replacing the organized P wave. Usually, paroxysmal AF (PAF) spontaneously terminates, differently from chronic AF (CAF), possibly due to the still-preserved main direction of the P-wave vector loop. To investigate this hypothesis, this study aims to evaluate the similarities between the P-wave vector loop and F-wave vector sway in subjects affected by PAF and CAF. Overall, 10-s VCG were acquired from 10 healthy (HEA) subjects showing normal sinus rhythm, 10 subjects affected by PAF (one during normal sinus rhythm and one during AF), and 10 subjects affected by CAF. P waves were extracted using ECGdeli software, while F waves were extracted after QRST cancellation. Ellipse axes and eccentricities were calculated as the root mean square of VCG components and the ratio between axes, respectively. Overall, 84 beats of HEA, 205 beats of PAF (89 beats during normal sinus rhythm and 116 during fibrillation), and 103 beats of CAF were analyzed. Distributions of axes and eccentricities of PAF are not statistically different (P-value>0.05) than normal sinus rhythm but features related to the Z axis of CAF were statistically lower than PAF (P-value$\langle 10^{-3}$). F-wave vector sway in PAF resembles the P-wave vector loop, suggesting the maintenance of the atrial depolarization main direction in subjects with self-terminating AF. Moreover, the F-wave vector sway is more manifest in PAF than in CAF.

Introduction

Atrial fibrillation (AF) is the most prevalent sustained cardiac arrhythmia globally, characterized by irregular and rapid atrial electrical activity [1]. It poses significant challenges in clinical management, considering the high variability in its first presentation and the presence of potential complications, such as stroke and heart failure [2,3].

Vectorcardiography (VCG) provides a spatial representation of the cardiac electrical activity in three dimensions, complementing the information obtained from standard electrocardiography (ECG). The application of VCG signal processing has facilitated the development of novel strategies for AF management and treatment [4–6]. Integrating signal processing algorithms with standard clinical systems can rapidly identify critical atrial arrhythmia patterns [7].

Studies have demonstrated the utility of VCG in characterizing atrial activity during AF. In healthy individuals, atrial electrical activity during normal sinus rhythm exhibits organized depolarization and repolarization patterns. The P wave reflects atrial depolarization, guiding atrial contraction and facilitating efficient blood flow into the ventricles [8,9]. The VCG provides a three-dimensional representation of atrial depolarization, in which P waves typically form a distinct vector loop, reflecting the direction and magnitude of the atrial depolarization vector. Changes in the morphology, size, or orientation of the VCG-based features may indicate atrial enlargement, conduction delays, or other pathological conditions affecting the atria [10].

In the presence of AF, the organized electrical activity is substituted by disordered and irregular impulses within the atria [11,12]. In the ECG, they lack a discernible morphology and exhibit variable amplitudes, frequencies, and directions, reflecting the disorganized atrial electrical activity of AF [8,13]. In the VCG they manifest as a continuous

* Corresponding author at: Department of Information Engineering, Università Politecnica delle Marche, via Brecce Bianche, 60131 Ancona, Italy.
E-mail address: l.burattini@univpm.it (L. Burattini).

https://doi.org/10.1016/j.jelectrocard.2025.153933

Available online 7 April 2025

non-reproducible movement of the atrial vector, not forming a distinct vector loop, in the following called AF vector sway or F-wave vector sway.

AF is classified into four types based on the duration and pattern of the episodes: paroxysmal, persistent, long-standing persistent, and permanent or chronic AF. Each AF type presents unique features and challenges in terms of management and treatment [14]. Specifically, paroxysmal AF (PAF) is characterized by episodes that start suddenly and typically resolve on their own within a short period, usually less than seven days; persistent AF usually lasts longer than a week, and it can stop spontaneously or may need cardioversion to restore sinus rhythm; long-standing persistent AF has lasted for more than a year and drugs and electrical cardioversion are unable to stop it, but ablation may restore normal sinus rhythm; eventually, permanent or chronic AF (CAF) is a stable condition where a clinical decision has been taken not to restore sinus rhythm, but only to control heart rate. The spontaneous termination of PAF episodes led us to the hypothesis that this might be due to the partial preservation of normal atrial depolarization, that appears covered by F waves. Vice versa, the persistent AF, long-standing persistent AF, and CAF may have increasingly lesser preservation of the normal atrial depolarization. This study aims to analyze the similarities of VCG P-wave vector loops and F-wave vector sways in PAF and to compare the F-wave vector sways in PAF versus CAF. If P-wave and F-wave shares similarities, it could indicate that the mechanisms underlying spontaneous termination involve the still-functioning portions of the normal atrial activity. Assumingly, a better characterization of the atrial depolarization could not only shed light on the pathophysiology of PAF but could be crucial for tailoring appropriate therapeutic strategies in the different AF types.

Methods

Database

Data of 30 digitized Holter recordings were retrospectively selected from the digital anonymized Holter database of the Studio Cardiologico Locati (Lombardy Region Authorization no. 2482 on Feb 25, 2003) obtained in 30 subjects selected as follows: 10 healthy (HEA) subjects presenting normal sinus rhythm, 10 subjects presenting short episodes of PAF, and 10 subjects presenting CAF. None of the subjects had a pacemaker/defibrillator implanted. All subjects had previously given their informed consent before data collection and acquisitions, which were undertaken in compliance with the ethical principles of the Helsinki Declaration and approved by the Institutional Ethic Committee. Anamnestic features are reported in Table 1. For each subject, a pseudo-orthogonal VCG was acquired during routine Holter screening using the Microport Spiderview recorder (sampling frequency: 200 Hz). Fig. 1 shows the electrode configuration for the measurements of the three

Table 1
Anamnestic features of the retrospectively recruited subjects.

	HEA		PAF		CAF	
	Age	Sex	Age	Sex	Age	Sex
1	23	F	70	M	87	F
2	36	F	72	F	88	M
3	61	F	100	F	76	M
4	71	F	76	M	70	M
5	70	F	81	F	86	F
6	82	M	70	M	82	F
7	87	F	68	M	90	M
8	69	F	58	F	83	F
9	33	M	86	F	85	F
10	77	M	64	F	74	F
TOT	61 ± 22	3 M/7F	75 ± 12	4 M/6F	82 ± 7	4 M/6F

CAF: chronic atrial fibrillation; F: female; HEA: healthy; M: male; PAF: paroxysmal atrial fibrillation.

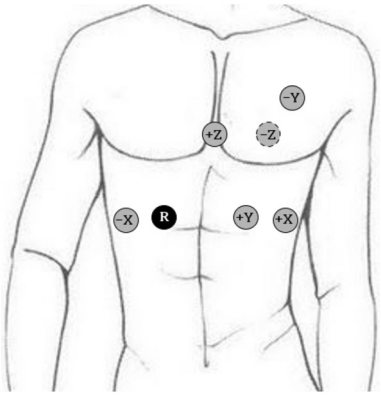

Fig. 1. Holter electrode configuration used for deriving the pseudo-orthogonal vectorcardiogram (VCG).

VCG components, that are X, corresponding to the right-left axis, Y, corresponding to the head-feet axis, and Z, corresponding to the back-front axis. For each HEA subject, a 10-s VCG was randomly selected. For each PAF subject, a 10-s VCG showing normal sinus rhythm and a 10-s VCG showing PAF were selected according to the clinical annotations, which were identified by a clinical equipe (Studio Cardiologico Locati) following the AF guidelines [1]. For each CAF subject, a 10-s VCG was randomly selected.

Vectorcardiogram processing

The flowchart of the VCG processing procedure is depicted in Fig. 2. The three VCG leads of each subject were prefiltered with a bidirectional 3rd-order bandpass Butterworth filter, with cut-off frequencies of 0.5 Hz and 40 Hz (Fig. 2.1), as a tradeoff between removing the typical interference of electrocardiographic Holter recording (e.g., baseline wander, motion artifacts, and electrode motion artifacts) while maintaining most spectral content of both P and F waves [15–17]. Then, the P waves during normal sinus rhythm (in both HEA and PAF subjects) and F waves during AF (in both PAF and CAF) were extracted (Fig. 2.2). Specifically, P waves were extracted by using the ECGdeli algorithm [18], an open-source delineator algorithm able to extract the onset and the end of the cardiac electrical waves. F waves were extracted by the temporo-spatial QRST cancellation techniques [19]. The F wave of each beat was defined as the 3-lead segment from 250 ms to 70 ms before each R-peak position, to match the same temporal location and resolution of the P wave. Finally, an 2D elliptic fit procedure was applied to all P and F waves (Fig. 2.3), by considering the three anatomical planes defined by the three VCG leads: frontal plane or X-Y plane, transverse plane or X-Z plane, and sagittal plane or *Z*-Y plane. The three ellipses of the three anatomical planes were fit using the least squares criterion [20].

Ellipse characterization

The VCG P-wave vector loop and F-wave vector sway were quantified in each anatomical plane using the ellipse features. Ellipses were characterized in terms of axes width (Fig. 3), which were the right-left axis (RL, μV), head-feet axis (HF, μV), and back-front axis (BF, μV). Moreover, the eccentricity of the ellipses for each plane was computed as:

$$ECC = \frac{\sqrt{M^2 - m^2}}{M} \quad (1)$$

where M and m are the major and the minor axes of the ellipse, respectively. Values of eccentricity close to 1 indicate an ellipse with a strong directionality (a line has an eccentricity equal to 1), while values of eccentricity close to 0 indicate an ellipse with a lack of directionality

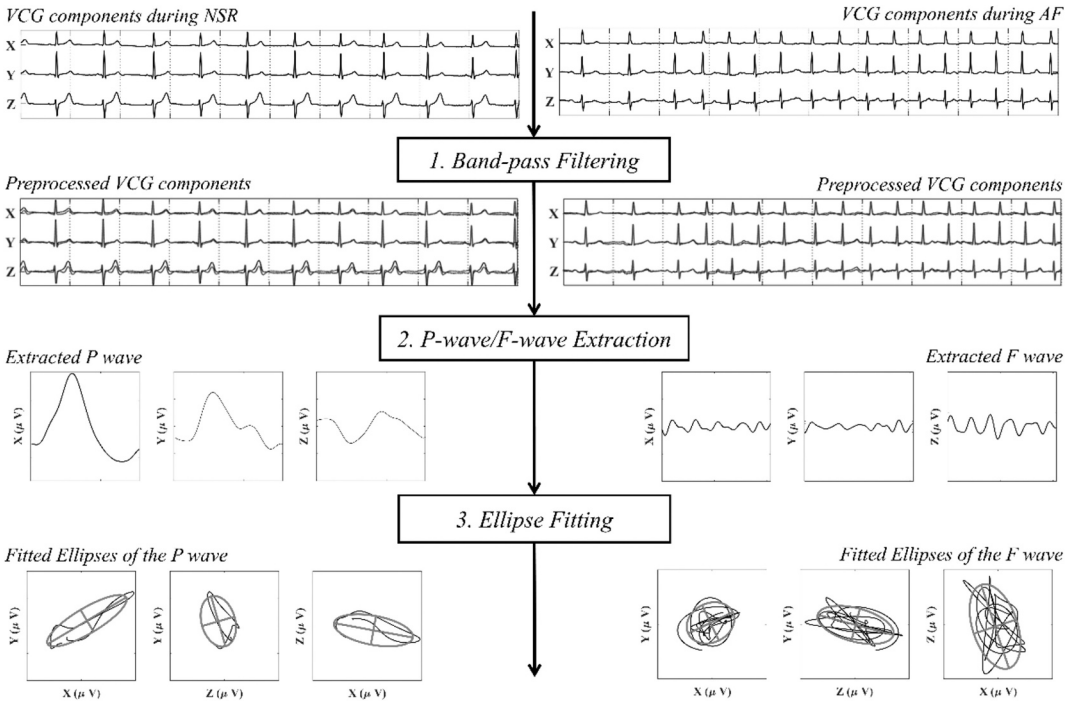

Fig. 2. Flowchart of vectorcardiogram (VCG) processing procedure applied to both P-wave in normal sinus rhythm (NSR) and F-wave in atrial fibrillation (AF).

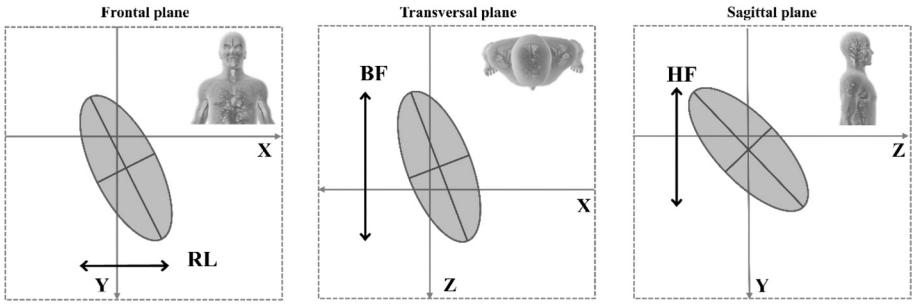

Fig. 3. Characterization of the ellipses in terms of axes width: right-left axis (RL), back-front axis (BF), and head-feet axis (HF) in a normal subject.

(a circle has an eccentricity of 0). ECC_F, ECC_T and ECC_S represent the eccentricities on the frontal plane, the eccentricity on the transverse plane, and the eccentricity on the sagittal plane, respectively.

Statistical analysis

The normality of feature distribution was evaluated by the Lilliefors test. Not normal distributions of axes and eccentricities of both P waves and F waves were quantified by 50th[25th;75th] percentiles. P-wave feature distributions of HEA were compared with those of PAF. Moreover, as inter-subject analysis, P-wave feature distributions were compared with F-wave feature distributions of PAF. Finally, the F-wave feature distributions of PAF were compared with those of CAF. Statistical comparisons were performed by paired Wilcoxon ranksum test for the equal median in intra-subject comparisons and by unpaired Wilcoxon ranksum test for the equal median in inter-subject comparisons. Statistical level (*P*-value) was set at 0.05.

Results

Overall, 84 P waves of HEA, 205 P and F waves of PAF (89 beats during normal sinus rhythm and 116 during PAF), and 103 F waves of CAF were analyzed. Fig. 4 displays examples of ellipse fitting of a P wave of HEA (Fig. 4.A), a P wave of PAF (Fig. 4.B), a segment of F waves of PAF (Fig. 4.C), and a segment of F wave of CAF (Fig. 4.D). P-wave and F-wave feature distributions are reported in Table 2. Differences in P-wave feature distributions of HEA and PAF were not statistically significant (*P-value* > 0.05), as well as P-wave and F-wave feature distributions of PAF. While F waves of PAF showed statistically higher HF (8.64 μV vs. 5.48 μV; *P-value* $\langle 10^{-3}$), ECC_F (0.91 vs. 0.87; *P-value* $< 10^{-7}$) and ECC_S (0.89 vs. 0.86; *P-value* $< 10^{-3}$) than F-waves of CAF.

Discussion

This study investigated the directionality of vector loop of P waves and vector sway of F waves, focusing on the comparison between the P-wave vector loop during normal sinus rhythm and F-wave vector sway in subjects with paroxysmal and chronic atrial fibrillation.

In vectorcardiography, P waves can be characterized as deterministic signals, and thus, being represented as distinct loops. On the contrary, the chaotic nature of atrial fibrillation does not allow us to recognize a single F-wave. The F waves depict vector sways in space, that can be characterized only in a global phenomenon. To compare the deterministic vector loop of P waves with the chaotic phenomenon of fibrillatory vector sway, three ellipses were used to quantify the main directions of these waves and compare them.

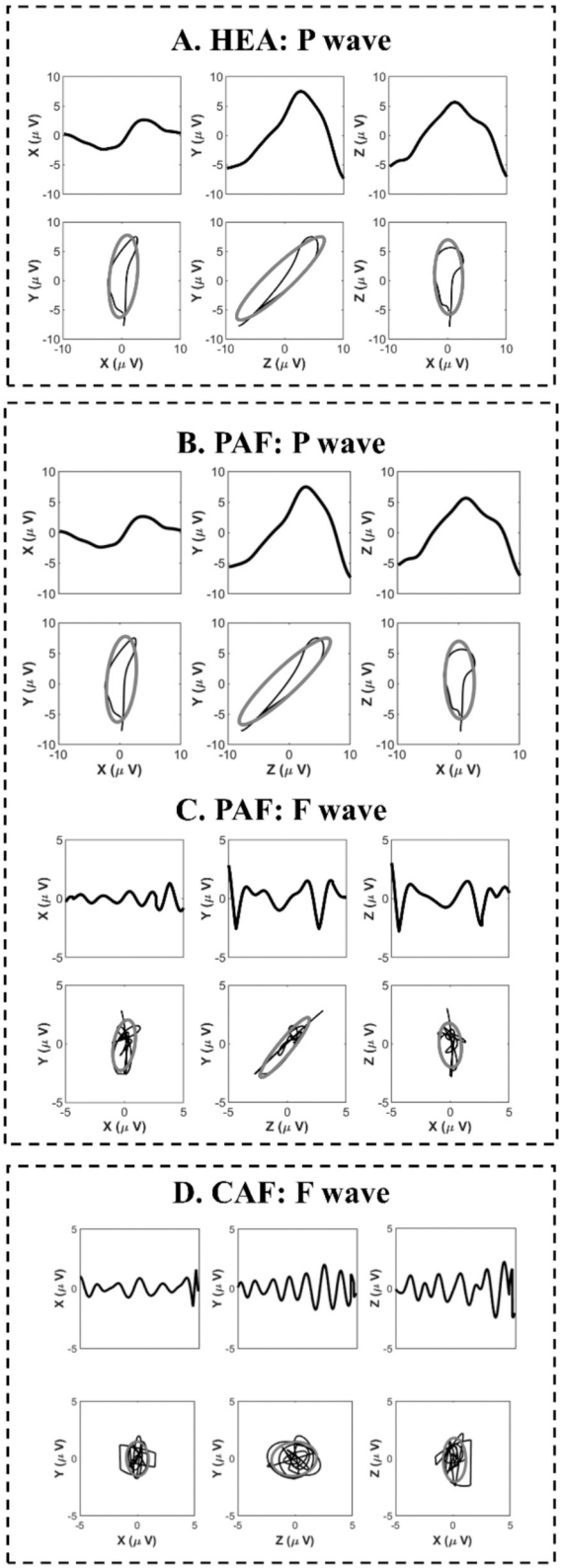

Fig. 4. Ellipse fitting. Panel A: example of a P wave of a healthy (HEA) subject during normal sinus rhythm. Panel B: example of a P wave of a subject affected by paroxysmal atrial fibrillation (PAF) during normal sinus rhythm. Panel C: example of a segment of F waves of a subject affected by paroxysmal atrial fibrillation (PAF) during a fibrillation episode. Panel D: example of a segment of F waves of a subject affected by chronic atrial fibrillation (CAF).

The results of this study underlined similarities and differences between the electrical atrial activity during normal sinus rhythm, PAF, and CAF, which may contribute to the understanding of the mechanisms underlying AF. Specifically, results suggest that the P-wave vector loops during normal sinus rhythm both in healthy subjects and in PAF subjects do not show significant differences. This evidence may be expected, considering that the episodes of AF selected in our PAF population were short, self-terminating, and asymptomatic. Moreover, this study showed that in PAF patients the F-wave vector sway presented no statistical difference with P-wave vector loop, supporting the hypothesis that parts of the healthy atrial depolarization pathway remain functional during PAF episodes. This finding may suggest that the mechanisms involved in spontaneous termination of PAF could be related to the partially still-functioning portions of atrial pathway. This finding could lead to improving the present diagnostic and therapeutic strategies, identifying patients with PAF with still preserved atrial activity that may benefit from trans-catheter ablation. Our results also showed that the F-wave vector sway of CAF patients was significantly different from that of PAF patients. Specifically, the Y-axis-related features in CAF patients were statistically lower than those observed in PAF patients, suggesting a reduction of the atrial electrical activity (typically pointing to superior-inferior and right-left directions) toward an undifferentiated shape in CAF. Indeed, the head-feet axis and the eccentricity values in the frontal and sagittal planes in CAF presented statistically significant reduced values. This evidence may indicate an increased degree of disorganization and a loss of integrity in the atrial excitation pathway, which could explain the permanent nature of CAF. Of note, this is in agreement with previous studies, that reported a greater spatial disorganization and variability in atrial electrical activity in CAF compared to PAF [21–23]. Finally, these findings also support the idea that AF stages represent distinct electrophysiological conditions, thus requiring different management and therapeutic approaches. Future research should further investigate such differences, also correlating the VCG features with the clinical characteristics of subjects (e.g., age, sex, presence of comorbidities, etc.) and atrial fibrillation history (e.g., duration of the episodes, frequency of recurrence, etc.). Moreover, examining post-ablation characteristics and outcomes may assess the effectiveness of different therapeutic strategies and different ablation techniques.

Our study was based on a beat-to-beat analysis, thus not investigating the beginning of atrial fibrillation episodes. Characterizing the eccentricity of the first beat of atrial fibrillation could be important to understanding the mechanisms and site of PAF onset. Detailed studies on the initial beats of PAF, compared with the pathway of the sinus beat in the same subject could reveal critical insights into the mechanisms triggering the arrhythmia. Identifying these initiation patterns could also aid in early detection and intervention, potentially preventing the progression to more severe forms.

Moreover, our work showed the feasibility of the QRST cancellation method, selecting only segments before the R peak for the analysis of F waves during AF. A further improvement could be to be use F waves all along the entire heartbeat. Thus, future research should evaluate the application of multiple F-wave extraction algorithms, to investigate if this might lead to more comprehensive characterizations of atrial fibrillation. Finally, investigating the potential use of machine learning and artificial intelligence in analyzing these data [24] could lead to more accurate and automatic detection of F waves, enhancing clinical decision-making and patient outcomes.

Limitations

The study presents several limitations, including the retrospective selection of subjects, the relatively small dataset, and the short recording durations, chosen to ensure the presence of self-terminating PAF episodes. The limited sample size and recording length may restrict the generalizability of the findings and their applicability to a broader patient population. Moreover, it does not allow the study of personalized F-

Table 2
P-wave and F-wave feature distributions, reported by $50^{th}[25^{th};75^{th}]$ percentiles.

		N° of beats	RL (μV)	HF (μV)	BF (μV)	ECC_F	ECC_T	ECC_S
HEA	*P wave*	84	9.58 [8.25;12.35]	12.22 [9.76;16.37]	6.72 [5.91;10.73]	0.95 [0.89;0.98]	0.89 [0.85;0.91]	0.91 [0.87;0.95]
PAF	*P wave*	89	11.08 [9.47;18.43]	11.79 [6.02;20.31]	6.02 [4.65;8.96]	0.95 [0.93;0.98]	0.92 [0.86;0.99]	0.87 [0.84;0.97]
	F wave	116	9.01 [6.93;15.49]	8.64† [7.62;10.27]	7.07 [4.10;9.63]	0.91† [0.86;0.95]	0.95 [0.86;0.97]	0.89† [0.86;0.94]
CAF	*F wave*	103	8.95 [5.08;15.09]	5.48† [3.64;9.78]	5.92 [3.33;8.1]	0.87† [0.77;0.89]	0.88 [0.86;0.9]	0.86† [0.84;0.88]

* $P < 0.05$; when comparing P-wave feature distributions of NSR with those of PAF; § $P < 0.05$; when comparing P-wave feature distributions with F-wave feature distributions of PAF; † $P < 0.05$; when comparing F-wave feature distributions of PAF with those of CAF.
BF: back-front axis; CAF: chronic atrial fibrillation; ECC_F: eccentricity on the frontal plane; ECC_S: eccentricity on the sagittal plane; ECC_T: eccentricity on the transverse plane; HEA: healthy; HF: head-feet axis; PAF: paroxysmal atrial fibrillation; RL: right-left axis.

wave characterization. Expanding the dataset and increasing recording durations in future studies will be crucial for validating these findings and enhancing their generalizability.

Of note, our data were collected under real-life conditions by 3-lead Holter recording by pseudo-orthogonal lead configuration (due to the impossibility of orthonormal lead acquisition, the direction of the lead vector was verified) and with reduced sampling frequency (i.e., 200 Hz). Thus, these results may not be readily applicable to the standard 12-lead 10-electrode ECG recording. Thus, future works are needed to explore the feasibility of using ECG-VCG conversion matrices to extend the applicability of this approach to standard 12-lead recordings, and thus, to assess the method in the clinical practice (e.g., pulmonary vein isolation ablation). Moreover, to efficiently remove ECG interferences, we decided to apply a low-pass filter at 40 Hz, which restricts the bandwidth of the analyzed signals (according to the guidelines, diagnostic information of the ECG requires a bandwidth up to 150 Hz, or even up to 250 Hz in some specific cases as in children). Consequently, this study concentrated on the low-frequency aspects of the P waves and F sways, differently from what is typically done in P-wave averaging studies [25–27]. Future studies will possibly compare both approaches, and see if they provide complementary information.

Finally, by definition, our method is based on the three ellipses as 2D temporo-spatial representation of the atrial activity. In spite of that, in this work, the role of the temporal component was not deeply investigated; thus, future studies will investigate the effect of wave duration, conduction velocity, heart rate, and shape variability on VCG P-wave and F-wave characterization.

Conclusion

The findings of this study suggest that the main direction of the atrial vector is preserved in paroxysmal but not in chronic atrial fibrillation, suggesting the maintenance of a normal vectorcardiographic P-wave vector loop in subjects with self-terminating atrial fibrillation. On the contrary, the shape of the F-wave vector sway in chronic atrial fibrillation indicates degeneration of the atrial electrical activity toward an undifferentiated shape. These findings may be helpful for more targeted and effective treatments for atrial fibrillation, by providing a patient-specific therapeutic approach.

CRediT authorship contribution statement

Agnese Sbrollini: Writing – original draft, Validation, Software, Methodology, Investigation, Formal analysis, Conceptualization. **Massimo W. Rivolta:** Writing – review & editing, Validation, Software, Methodology, Formal analysis. **Peter Van Dam:** Writing – review & editing, Visualization, Validation, Methodology, Formal analysis. **Elisabetta Viani:** Writing – review & editing, Visualization, Resources, Data curation. **Micaela Morettini:** Writing – review & editing, Visualization, Resources. **Roberto Sassi:** Writing – review & editing, Supervision, Resources, Funding acquisition, Formal analysis. **Laura Burattini:** Writing – review & editing, Supervision, Resources, Project administration, Formal analysis, Conceptualization. **Emanuela T. Locati:** Writing – review & editing, Validation, Resources, Project administration, Formal analysis, Data curation.

Declaration of competing interest

The authors report no conflict of interest.

References

[1] Cheung CC, Nattel S, Macle L, Andrade JG. Management of atrial fibrillation in 2021: an updated comparison of the current CCS/CHRS, ESC, and AHA/ACC/HRS guidelines. Can J Cardiol 2021;37:1607–18.
[2] Gillis AM. Atrial fibrillation and ventricular arrhythmias: sex differences in electrophysiology, epidemiology, clinical presentation, and clinical outcomes. Circulation 2017;135:593–608.
[3] Nattel S. Atrial electrophysiology and mechanisms of atrial fibrillation. J Cardiovasc Pharmacol Ther 2003;8:S5–11.
[4] Vondrak J, Penhaker M. Review of processing pathological vectorcardiographic records for the detection of heart disease. Front Physiol 2022;13:856590.
[5] Filos D, Chouvarda I, Tachmatzidis D, Vassilikos V, Maglaveras N. Beat-to-beat P-wave morphology as a predictor of paroxysmal atrial fibrillation. Comput Methods Programs Biomed 2017;151:111–21.
[6] Carlson J, Havmöller R, Herreros A, Platonov P, Johansson R, Olsson B. Can orthogonal lead indicators of propensity to atrial fibrillation be accurately assessed from the 12-lead ECG? EP Europace 2005;7:S39–48.
[7] Narayan SM, Feld GK, Hassankhani A, Bhargava V. Quantifying Intracardiac Organization of Atrial Arrhythmias Using Temporospatial Phase of the electrocardiogram. J Cardiovasc Electrophysiol 2003;14:971–81. https://doi.org/10.1046/j.1540-8167.2003.03213.x.
[8] Allessie MA, Boyden PA, Camm AJ, Kléber AG, Lab MJ, Legato MJ, et al. Pathophysiology and prevention of atrial fibrillation. Circulation 2001;103:769–77.
[9] Klabunde R. Cardiovascular physiology concepts. Lippincott Williams & Wilkins; 2011.
[10] Locati ET, Pappone C, Heilbron F, van Dam PM. CineECG provides a novel anatomical view on the normal atrial P-wave. Europ Heart J Digit Health 2022;3:169–80.
[11] Schotten U, Verheule S, Kirchhof P, Goette A. Pathophysiological mechanisms of atrial fibrillation: a translational appraisal. Physiol Rev 2011;91:265–325.
[12] de Groot NMS, Houben RPM, Smeets JL, Boersma E, Schotten U, Schalij MJ, et al. Electropathological substrate of longstanding persistent atrial fibrillation in patients with structural heart disease: epicardial breakthrough. Circulation 2010;122:1674–82.
[13] Sbrollini A, Marcantoni I, Morettini M, Burattini L. Spectral F-wave index for automatic identification of atrial fibrillation in very short electrocardiograms. Biomed Sign Process Control 2022;71:103210. https://doi.org/10.1016/j.bspc.2021.103210.
[14] Lip GYH, Fauchier L, Freedman SB, Van Gelder I, Natale A, Gianni C, et al. Atrial fibrillation (primer). Nat Rev Dis Primers 2016:2.
[15] Hiraki T, Ikeda H, Ohga M, Kubara THI, Yoshida T, Ajisaka H, et al. Frequency- and time-domain analysis of P wave in patients with paroxysmal atrial fibrillation. Pacing Clin Electrophysiol 1998;21:56–64. https://doi.org/10.1111/j.1540-8159.1998.tb01061.x.
[16] Raygor VP, Ng J, Goldberger JJ. Surface ECG f wave analysis of Dofetilide drug effect in the atrium. J Cardiovasc Electrophysiol 2015;26:644–8. https://doi.org/10.1111/jce.12645.
[17] Sbrollini A, Marcantoni I, Morettini M, Burattini L. Spectral F-wave index for automatic identification of atrial fibrillation in very short electrocardiograms. Biomed Sign Process Control 2022;71:103210.
[18] Pilia N, Nagel C, Lenis G, Becker S, Dössel O, Loewe A. ECGdeli - an open source ECG delineation toolbox for MATLAB. SoftwareX 2021;13:100639. https://doi.org/10.1016/j.softx.2020.100639.
[19] Stridh M, Sornmo L. Spatiotemporal QRST cancellation techniques for analysis of atrial fibrillation. IEEE Trans Biomed Eng 2001;48:105–11.

[20] Prasad DK, Leung MKH, Quek C. ElliFit: an unconstrained, non-iterative, least squares based geometric ellipse fitting method. Pattern Recogn 2013;46:1449–65.
[21] Botteron GW, Smith JM. Quantitative assessment of the spatial organization of atrial fibrillation in the intact human heart. Circulation 1996;93:513–8.
[22] Cervigón R, Moreno J, Reilly RB, Millet J, Pérez-Villacastín J, Castells F. Entropy measurements in paroxysmal and persistent atrial fibrillation. Physiol Meas 2010; 31:1011.
[23] Gaita F, Calò L, Riccardi R, Garberoglio L, Scaglione M, Licciardello G, et al. Different patterns of atrial activation in idiopathic atrial fibrillation: simultaneous multisite atrial mapping in patients with paroxysmal and chronic atrial fibrillation. J Am Coll Cardiol 2001;37:534–41.
[24] Goffi L, Sbrollini A, Mortada MJ, Morettini M, Laura Burattini. A novel deep-learning method for fibrillatory waves extraction. Comput Cardiol 2010:2022.
[25] Stafford P, Denbigh P, Vincent R. Frequency analysis of the P wave: comparative techniques. Pacing Clin Electrophysiol 1995;18:261–70.
[26] Alcaraz R, Martínez A, Rieta JJ. Role of the P-wave high frequency energy and duration as noninvasive cardiovascular predictors of paroxysmal atrial fibrillation. Comput Methods Programs Biomed 2015;119:110–9.
[27] Zink MD, Laureanti R, Hermans BJM, Pison L, Verheule S, Philippens S, et al. Extended ECG improves classification of paroxysmal and persistent atrial fibrillation based on P-and f-waves. Front Physiol 2022;13:779826.